J Mol Model (2013) 19:2855–2864
DOI 10.1007/s00894-012-1729-0

ORIGINAL PAPER

Computational study on C−H···π interactions of acetylene with benzene, 1,3,5-trifluorobenzene and coronene

Tandabany C. Dinadayalane · Guvanchmyrat Paytakov · Jerzy Leszczynski

Received: 7 October 2012 / Accepted: 12 November 2012 / Published online: 18 December 2012

Abstract Meta-hybrid density functional theory calculations using M06-2X/6-31+G(d,p) and M06-2X/6-311+G(d,p) levels of theory have been performed to understand the strength of C−H···π interactions of two possible types for benzene-acetylene, 1,3,5-trifluorobenzene-acetylene and coronene-acetylene complexes. Our study reveals that the C−H···π interaction complex where acetylene located above to the center of benzene ring (classical T-shaped) is the lowest energy structure. This structure is twice more stable than the configuration characterized by H atom of benzene interacting with the π-cloud of acetylene. The binding energy of 2.91 kcal/mol calculated at the M06-2X/6-311+G(d,p) level for the lowest energy configuration (**1A**) is in very good agreement with the experimental binding energy of 2.7±0.2 kcal/mol for benzene-acetylene complex. Interestingly, the C−H···π interaction of acetylene above to the center of the aromatic ring is not the lowest energy configuration for 1,3,5-trifluorobenzene-acetylene and coronene-acetylene complexes. The lowest energy configuration (**2A**) for the former complex possesses both C−H···π interaction and C−H···F hydrogen bond, while the lowest energy structure for the coronene-acetylene complex involves both π-π and C−H···π interactions. C−H stretching vibrational frequencies and the frequency shifts are reported and analyzed for all of the configurations. We observed red-shift of the vibrational frequency for the stretching mode of the C-H bond that interacts with the π-cloud. Acetylene in the lowest-energy structures of the complexes exhibits significant red-shift of the C−H stretching frequency and change in intensity of the corresponding vibrational frequency, compared to bare acetylene. We have examined the molecular electrostatic potential on the surfaces of benzene, 1,3,5-trifluorobenzene, coronene and acetylene to explain the binding strengths of various complexes studied here.

Keywords C−H···π interactions · π-π interactions · 1,3,5-trifluorobenzene · Acetylene · Hydrogen bond · Density functional theory · Vibrational frequency shift

Introduction

Noncovalent interactions involving aromatic systems or those between aromatic moieties have been the subject of intensive studies over the past three decades because of their importance for the binding properties of nucleic acids, the stability of proteins, and the binding affinities in host-guest chemistry [1–8]. They are also vital in the area of materials science [1, 2, 9, 10]. The interactions such as π–π, C−H···π, N−H···π, O−H···π, S···π, cation-π, halogen bonding and hydrogen bonding stimulate both experimental and computational interest [1–5, 11–23]. The C−H···π interactions play important role in crystal packing and in molecular recognition for numerous ligand binding proteins [6–8, 24]. In our group, we have recently studied π–π, C−H···π and cation-π interactions involving benzene and ring-fused benzene systems using high-level ab initio and DFT methods [13–20]. Very weak, noncovalent interactions dominated by dispersion forces (for example, π–π, C−H···π interactions) have been a great challenge for both experiment and theory [1–3, 25–36].

Benzene dimer has received tremendous attention due to being the simplest prototype system for π–π and C−H···π

We are honored to have an opportunity to contribute this manuscript to the special Politzer Issue. In addition to be influenced for many years by Peter's outstanding contributions to science, we have also been privileged to possess his friendship. We wish Peter many, many more prolific and healthy years!

T. C. Dinadayalane · G. Paytakov · J. Leszczynski (✉)
Interdisciplinary Center for Nanotoxicity,
Department of Chemistry and Biochemistry,
Jackson State University, 1400 J. R. Lynch Street,
Jackson, MS 39217, USA
e-mail: jerzy@icnanotox.org

T. C. Dinadayalane
e-mail: dina@icnanotox.org

interactions [15, 16, 25–33] and also it was considered as a good model for π−π interactions in proteins [4]. Experimental and theoretical studies evidence the C−H···π interactions in the T-shaped configuration of the benzene dimer [15, 16, 25–33]. Theoretical studies [15, 34] reproduced the red shifts of C−H stretching frequencies reported by experiments [35, 36] for the bent-T shaped configuration of benzene dimer. Hobza and Havlas investigated the C−H···π interactions in different complexes such as CH_4···benzene, Cl_3CH···benzene, and NCH···benzene. They calculated binding energies for the complexes and the frequency shifts corresponding to the interacting C−H bonds [37]. Kwac et al. have studied the C−H···π interactions in the T-shaped structure of phenol-benzene complexes using quantum chemical calculations, molecular dynamics simulations and IR spectroscopy [12]. The accurate interaction energy was reported in the gas phase for the C−H···π interactions of the benzene-methane model system by both experiment and theory. The binding energy estimated using CCSD(T) approach at the basis set limit (D_e) was 1.43 kcal/mol. However, the calculated binding energy (D_0) after the zero-point vibrational energy correction was reported as 1.13 kcal/mol, which is in excellent agreement with the experimental result of 1.03–1.13 kcal/mol [38].

Using very accurate coupled-cluster theory calculations, Sherrill and co-workers investigated the methane-benzene, methane-phenol, and methane-indole complexes. They revealed that the additional electron density provided by the π system of the upper benzene of the T-shaped benzene dimer is important in stabilizing aromatic C−H···π interactions over aliphatic C−H···π interactions in case of methane-benzene complex [39]. C_6H_6-$(C_4H_2)_n$ complexes with n=1 and 2 were obtained experimentally and C−H···π interactions were characterized between diacetylene and benzene in those complexes using ultraviolet and infrared spectroscopy. Computational studies using *ab initio* and DFT methods complemented the experimental results [40]. The acetylene–benzene complex is a prototype system for the investigation of the characteristics of C−H···π interactions [41]. The crystal structure of the above-mentioned complex was already reported [42]. A recent theoretical study has focused on the X−H (X=C, Cl and Br) bonding strength and the vibrational frequency shift (classical red-shift or improper blue-shift) for a range of model complexes involving X−H···π interactions [43]. Tsuzuki and co-workers have investigated the C−H···π interactions in benzene-ethylene and benzene-acetylene complexes. The C−H···π interaction in the latter complex was reported to be significantly different from that of benzene-ethylene and benzene-methane complexes. The reported experimental binding energies (D_0) for the benzene-ethylene and benzene-acetylene complexes are 1.4±0.2 and 2.7±0.2 kcal/mol, respectively [44].

Mishra et al. have recently reported a systematic study of the influence of multiple fluoro-/methyl substitution to benzene on C−H···π interactions involving acetylene. Furthermore, they have assessed the performance of various recently developed density functional theory methods for calculations of such interactions. They concluded that M05-2X, M06-2X and ωB97X-D methods are best performers based on the reference of estimated CCSD(T)/CBS results [45]. Infrared spectroscopy for C−H stretching vibrations of benzene-acetylene and several aromatics-acetylene clusters was reported experimentally [41]. Sundararajan et al. investigated C−H···π interactions in benzene-acetylene complex using both computation and experiment. They have explored both possibility: C-H of acetylene interacts with aromatic π-cloud of benzene and C−H group of benzene interacts with π-electrons of acetylene [46]. It is well known that the H atoms of the acetylene molecule form C−H···π interactions with the π-system of the arene rings. Very recently, crystal structure study has shown the other possibility of C−H···π contacts: The H atom bonded to an aromatic C atom interacts with the electron cloud of an acetylenic C−C bond [24].

In this paper, we have systematically studied the C−H···π interactions between acetylene and the aromatic π-system (benzene, 1,3,5-trifluorobenzene [TFB], coronene). Scheme 1 depicts the structures of model systems considered in this study. We took into account both possibilities: (i) C−H of acetylene interacts with aromatic π-cloud, and (ii) C−H of aromatic system interacts with π-electrons of acetylene (for model see Scheme 1). Our aim is to understand the binding strength of these two kinds of C−H···π interactions and to explain how the C−H···π interactions vary by modifying the π-system of benzene. We have considered one example for substituted (three F substitution—1,3,5-trifluorobenzene) and one example for ring fused benzene system (coronene). The latter system allows us to explore the C−H···π interactions of acetylene with the six-membered ring at the center as well as at the edge. Coronene may be considered as the simplest model system for graphene. Hence, the interactions of metals or organic species with coronene have been the subject of recent theoretical interest [47–49].

Computational details

All the calculations of geometry optimizations and vibrational frequencies in this work were performed using the Gaussian 09 suite of programs [50]. A range of starting geometries was chosen to explore various configurations of the considered complexes. The structures of different configurations of the complexes and the individual fragments were fully optimized using the M06-2X/6-31+G(d, p) and M06-2X/6-311+G(d,p) levels. Harmonic vibrational frequency calculations were performed for all the optimized

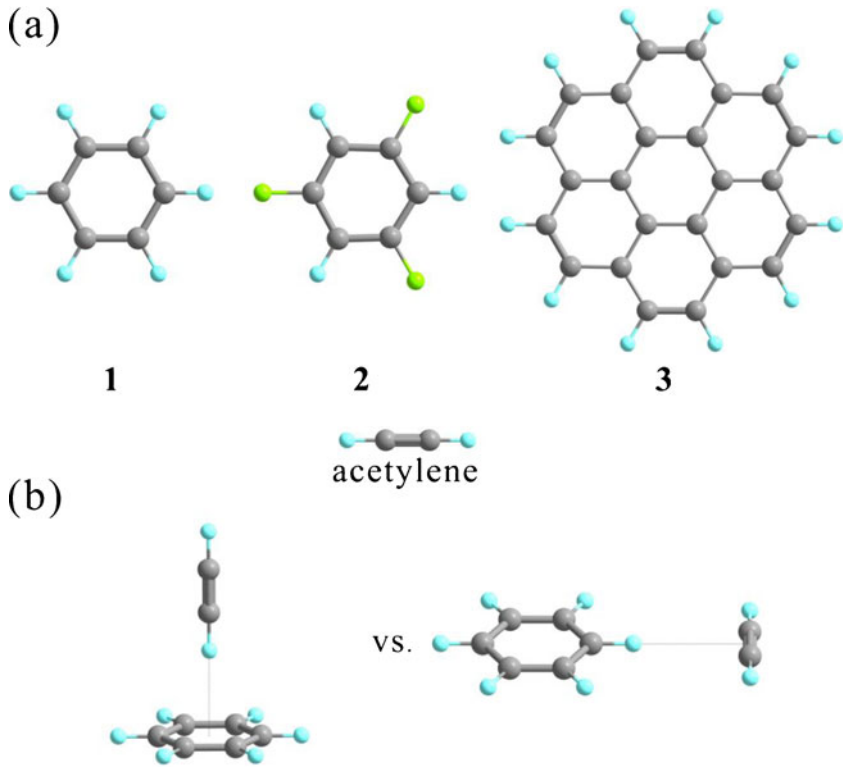

Scheme 1 **a** Structures of benzene (1), 1,3,5-trifluorobenzene (2), coronene (3), acetylene. **b** The model system for interaction of C−H of acetylene with aromatic π cloud vs. the interaction of the C−H of aromatic system with the π electrons of acetylene

geometries to assess the nature of stationary points. The vibrational frequency calculations are useful to characterize the C−H stretching frequency of the C−H···π interactions in the complexes and also to examine the frequency shift (either red or blue shift) of these stretching modes with respect to the free monomer. Binding energies were corrected for basis set superposition error (BSSE) using the counterpoise procedure proposed by Boys and Bernardi [51]. We have adopted the Mulliken charges of acetylene fragment in each of the complexes to analyze any charge transfer between their two components. Recently, Mishra et al. have reported very good performance of M06-2X functional for similar kind of C−H···π interactions involving acetylene with various substituted benzene systems [45]. Hence, the theoretical levels employed in our study are adequate to obtain very reliable results. Molecular electrostatic potential (MESP) maps were generated using density predicted at the M06-2X/6-311+G(d,p) level for benzene, 1,3,5-trifluorobenzene, coronene and acetylene. The electrostatic potentials were mapped on the surface of the electron density of the 0.002 unit. Spartan 10 software was used for the calculations of molecular electrostatic potentials and to produce the MESP pictures [52, 53].

Results and discussion

Figure 1 depicts the structures with important geometrical parameters for three lowest energy configurations of benzene-acetylene complex (**1A**-**1C**), three lowest energy configurations of 1,3,5-trifluorobenzene-acetylene complex (**2A**–**2C**) and six lowest energy configurations of coronene-acetylene complex (**3A**–**3F**). We have considered several possible structures for each of the complexes. Acetylene stands upright above to the center of the six-membered ring in case of **1A**, **2B** and **3B**. However, in case of **3F**, the acetylene is located above the edge six-membered ring of coronene with slightly bent T-shaped structure. For the above-mentioned four configurations, the hydrogen of acetylene binds with the π-cloud. In this scenario, the C−H bond of acetylene is treated as the hydrogen bond donor in a C−H···π H-bond. The aromatic C−H interacts with the π-electrons of acetylene in all the remaining configurations except **3A** where both π-π and C−H···π type of interactions coexist. The structure **3A** was obtained by following the normal mode of the imaginary frequency obtained for **3F**. Monodentate type of C−H···π interaction is observed in case of **1C**, **2C** and **3E**, whereas bidentate type is seen for **1B**, **3C** and **3D**. Structure **2A** is unique since it has both C−H···π and C−H···F hydrogen bond interactions.

Calculated binding energies for different configurations of the complexes are listed in Table 1. We also provide the charge of acetylene in the complex. The binding energy trends obtained at the M06-2X/6-31+G(d,p) and M06-2X/6-311+G(d,p) levels are exactly the same. It should be mentioned that the values of binding energies also do not considerably vary between these two levels. It is very clear from the data given in Table 1 that substitution of three

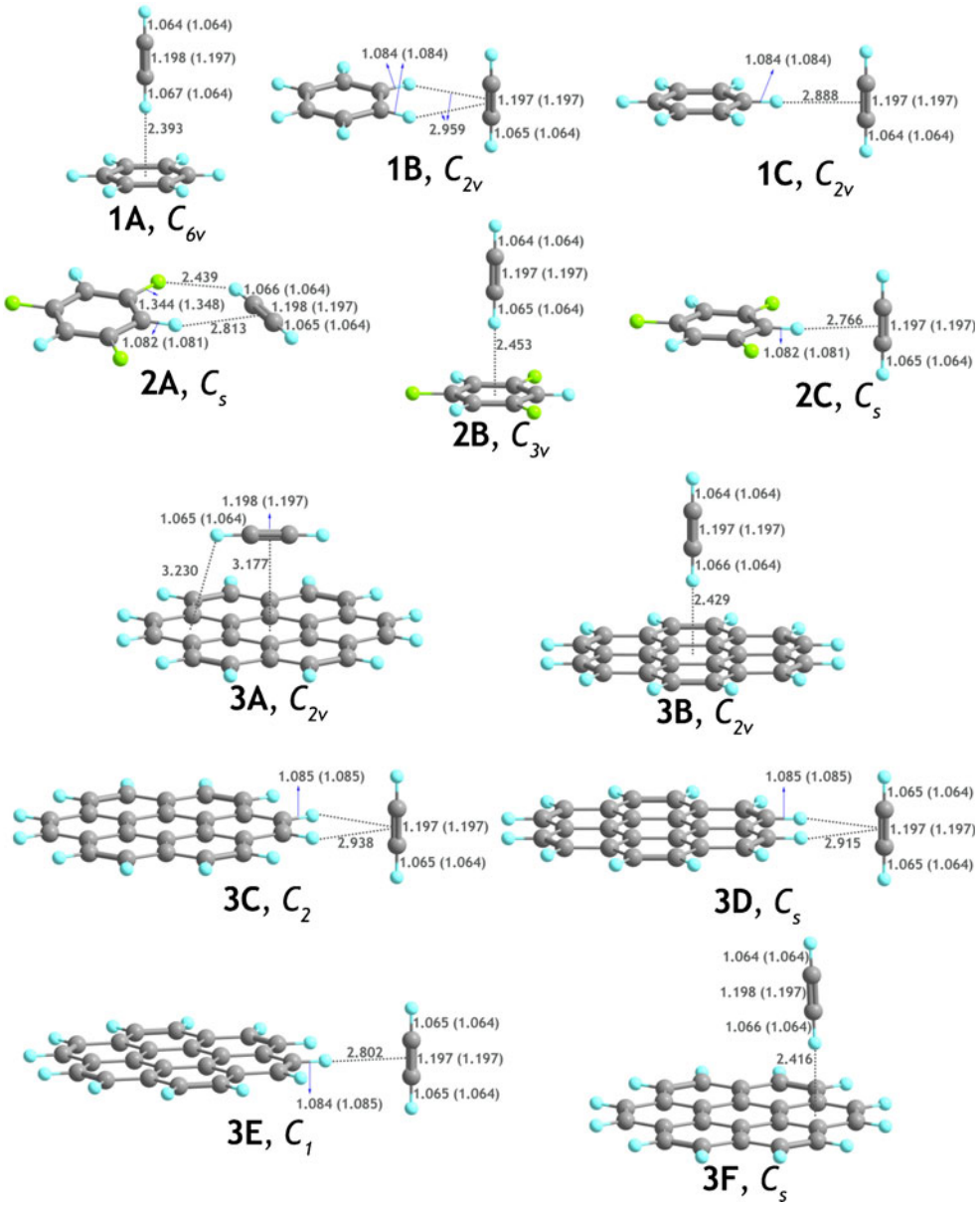

Fig. 1 Important bond distances and selected distances between the fragments (in Å) obtained at the M06-2X/6-311+G(d,p) level. The values given in parentheses correspond to the monomer unit before complexation

H atoms by fluorine atoms or fusion of rings to all the C−C bonds of benzene significantly affects the strength of C−H···π interactions. The configuration involving C−H of acetylene binding to the π-cloud of aromatic ring is not the lowest energy structure in case of 1,3,5-trifulorobenzene-acetylene and coronene-acetylene complexes.

The binding energy for **1A** (2.91 kcal/mol) is significantly larger than that of **1B** (1.40 kcal/mol) and **1C** (0.52 kcal/mol). The configuration (**1B**) with two aromatic hydrogen atoms interacting with π-electrons of acetylene is more preferred than the configuration with monodentate type binding (**1C**). In case of **1A**, acetylene is a proton donor; H of acetylene interacts with the π-cloud of benzene. Although both **1A** and **1B** are characterized by all-positive vibrational frequencies, **1B** is a local minimum with smaller binding energy compared to **1A**. This is in consistent with the earlier study by Sundararajan et al. [46]. The binding energy of 2.91 kcal/mol calculated at the M06-2X/6-311+G(d,p) level for **1A** is in very good agreement with the experimental binding energy of 2.7±0.2 kcal/mol for benzene-acetylene complex [44]. Shaibasaki et al. have estimated the CCSD(T) interaction energies of 2.8 kcal/mol [44], while the recent study by Mishra et al. has shown the value of 2.70 kcal/mol estimated at the CCSD(T)/CBS [45]. It should be noted that the CCSD (T) calculations are much more expensive than the density functional theory calculations at the M06-2X/6-311+G(d,p) level. The latter level yields the binding energy very close to the experimental as well as to very expensive CCSD(T) computational results. The binding

Table 1 Calculated binding energies (in kcal/mol) for the benzene-acetylene (Benzene-Ac), 1,3,5-trifluorobenzene-acetylene (TFB-Ac) and coronene-acetylene (Coronene-Ac) complexes at two different levels. The binding energies include the basis set superposition error (BSSE) correction. Charge (q, in e$^-$) of acetylene fragment in the complex is also given

Benzene-Ac				TFB-Ac				Coronene-Ac			
Conf.[a]	I[b]	II[c]	q[d]	Conf.[a]	I[b]	II[c]	q[d]	Conf.[a]	I[b]	II[c]	q[d]
1A	2.82	2.91	+0.070	2A	1.76	1.85	+0.024	3A	3.10	3.36	−0.038
1B	1.34	1.40	+0.012	2B	1.20	1.31	+0.090	3B	1.78	1.80	+0.003
1C	0.75	0.52	+0.008	2C	1.08	1.03	+0.014	3C	1.56	1.56	+0.028
								3D	1.49	1.53	+0.039
								3E	1.48	1.48	+0.020
								3F	2.14	2.12	+0.024

[a] Different configurations of the complex

[b] The values obtained at the M06-2X/6-31+G(d,p) level

[c] The values obtained at the M06-2X/6-311+G(d,p) level

[d] Total charge of acetylene species in the complex obtained at the M06-2X/6-311+G(d,p) level

energy obtained for **1A** is slightly more than the results of the C−H···π interactions (T-shaped or bent-T shaped configurations) in the benzene dimer [15, 16, 25–30].

Tsuzuki and co-workers pointed out that both electrostatic and dispersion interactions play important role in stabilization of the benzene-acetylene complex of **1A**. Furthermore, the large electrostatic contribution was related to the activation of C−H bond of acetylene and thus, the intermolecular interaction was treated as π-hydrogen-bond-like [44]. As suggested by one of the reviewers following the importance of electrostatics in these types of complexes, we have looked at the electrostatic potentials on the molecular surfaces of benzene, 1,3,5-trifluorobenzene, coronene and acetylene (Fig. 2). Significantly larger positive potential (see Fig. 2) of acetylenic hydrogen atoms compared to benzene hydrogen atoms explains that the binding energy for **1A** is greater than those predicted either for **1B** or **1C**. The distance between the interacting H atom and the center of benzene in **1A** at the M06-2X/6-311+G(d,p) level (2.393 Å) is longer than that reported at the MP2/aug-cc-pVDZ level (2.283 Å) [44].

2A complex exhibits stronger binding than **2B** and **2C**. This is due to the existence of both C−H···π and C−H···F hydrogen bonds in case of **2A**. As shown in Fig. 2, the positive and negative potentials correspondingly for H and F atoms in 1,3,5-trifluorobenzene strongly support the double interaction of C−H···π and C−H···F hydrogen bonds in case of **2A**. The structure **2A** is more stabilized (by 0.54 kcal/mol) than **2B**. It should be noted that configuration **2B** has been studied in the recent computational investigation [45]. The binding energy for **2B** at the M06-2X/6-311+G(d,p) level is 1.31 kcal/mol that is very close to the estimated CCSD(T)/CBS value of 1.38 kcal/mol [45]. This again indicates the excellent performance of M06-2X/6-311+G (d,p) level for these types of complexes involving C−H···π interactions. The distance between interacting H of acetylene and the center of six-membered ring of 1,3,5-trifluorobenzene reported at the MP2/aug-cc-pVDZ level is 2.287 Å [45], which is considerably smaller than the value of 2.453 Å obtained at the M06-2X/6-311+G(d,p) level. The complexes **2C** and **1C** have the same type of C−H···π interactions where the H atom of aromatic ring is involved in the binding. The binding energy of **2C** is greater than that of **1C**. This could be explained by higher positive potential for the hydrogen atoms of 1,3,5-trifluorobenzene compared to the hydrogen atoms of benzene (Fig. 2). Large negative potential above and below the center of benzene ring compared to the ring of 1,3,5-trifluorobenzene explains that the binding energy for **1A** is greater than that of **2B**.

The structure **3A** is substantially more stable than other configurations in this category of coronene-acetylene complexes because it possesses both π-π and C−H···π interactions. As shown in Fig. 2, high positive potential of acetylenic hydrogen atoms and the high negative potential above and below the outer ring of coronene could evidence for C−H···π interactions in **3A**. The classical T-shaped configuration formed by the C−H of acetylene interacting with central ring of coronene (**3B**) and the edge ring of coronene (**3F** structure) are considerably less stable than **3A**. The complex **3B** has smaller binding energy (by 0.32 kcal/mol) than **3F**. The former one is a minimum, but the latter one is not. The negative potential above and below of the central ring is significantly lower compared to the edge ring. This explains why **3F** has larger binding energy than **3B**. In case of **3C**, **3D** and **3E**, the H of coronene (it is a proton donor) interacts with the π-electrons of acetylene. It is interesting to note that, unlike the case of benzene-acetylene complex, the difference in binding energies among these three

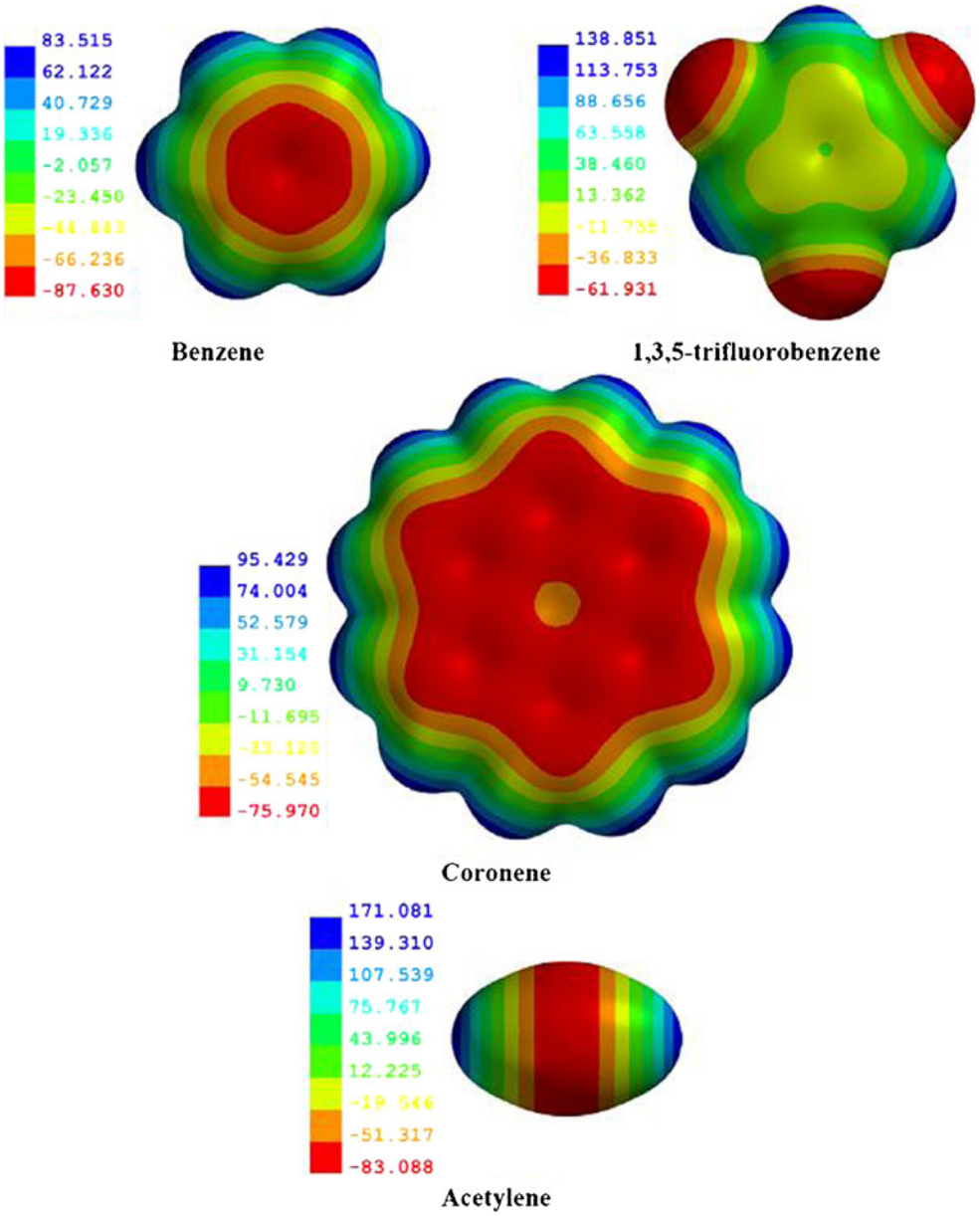

Fig. 2 Molecular electrostatic potential maps generated using density at the M06-2X/6-311+G(d,p) level for benzene, 1,3,5-trifluorobenzene, coronene and acetylene. Electrostatic potentials are mapped on the surface of the electron density of the 0.002 unit. The red surface corresponds to a region of negative electrostatic potential, whereas the blue color corresponds to the positive potential. The numbers of positive and negative potentials are given in kJ/mol

configurations is very small (< 0.09 kcal/mol). To the best of our knowledge, there is no experimental and/or theoretical data for coronene-acetylene complex to be compared in this paper. Figure 2 depicts that the hydrogen atoms of acetylene have higher positive potential than the hydrogen atoms of coronene. Therefore, the complexes **3B** and **3F** have larger binding energies than the complexes **3C**, **3D** and **3E**.

We have adopted the Mulliken charges for acetylene fragment in each of the complexes. As shown from the data provided in Table 1, the charge of acetylene in the complex is positive in all the cases, except **3A**. This positive charge indicates that the electron transfer takes place from acetylene molecule to the aromatic moiety in the complex. However, the electron charge of 0.038 e^- transferred from coronene to acetylene in case of **3A**. It is important to mention that there is no relationship between the charge of acetylene in the complex and the binding energies.

Configurations **1A**, **2B**, **3B** and **3F** have the C−H···π interactions of same type – H of acetylene binds directly above the center of aromatic six-membered ring. Among these four structures, the prototype benzene-acetylene complex (**1A**) shows stronger binding than other three. The distance between the interacting H atom of acetylene and the center of the six-membered ring involved in binding of acetylene is in good correlation with the binding energy. The complex with the shortest such distance has the highest binding energy and vice versa. The trend of binding energy is **1A** (2.91)>**3F** (2.12)>**3B** (1.80)>**2B** (1.31 kcal/mol) and the inter-moiety distance follows the trend **1A** (2.39)<**3F** (2.42)<**3B** (2.43)<**2B** (2.45 Å). The bond length of

interacting C−H is slightly elongated in all these four complexes. It should be mentioned that **3F** is characterized as transition state while other three structures are minima on their respective potential energy surface. However, **3F** exhibits stronger binding than **3B**. This could be attributed to more electron density at the edge ring than the central ring. As shown in Table 1, the charge of acetylene in **1A** and **2B** is notably higher than that in **3B** and **3F**. Thus, coronene-acetylene complex behaves different than benzene-acetylene and 1,3,5-trifulorobenzene-acetylene complexes. The bond length of C−H of acetylene in **3A** is elongated marginally (by 0.001 Å), compared to free acetylene. In majority of the configurations, the C−C bond length of acetylene remains the same as that of free acetylene. It is elongated to a small extend upon forming the clusters of **1A**, **2A**, **3A** and **3F** (see Fig. 1).

Previous study demonstrated that increasing the number of methyl substitution in benzene enhances the strength of C−H···π interactions between methane and benzene [54]. It was shown that increasing the number of methyl substitution increased the strength of C−H···π interactions between acetylene and benzene, but decreased the binding strength by increasing the number of fluoride substitution to benzene [45]. Such a behavior is different from the case of π-π stacking interactions where the binding strength enhanced by adding substituents regardless of their nature [55–60]. In the present paper, we clearly observe that the strength of C−H of acetylene interaction with the aromatic π-system considerably decreased in cases of TFB-acetylene and coronene-acetylene complexes with reference to benzene-acetylene. Interestingly, the difference in binding energy between two different binding modes (H of acetylene interacting with aromatic π-system versus H of aromatic system interacting with π-electrons of acetylene) decreases while we move from benzene-acetylene (reference system) to TFB-acetylene then to coronene-acetylene complexes.

IR frequencies: C−H stretching frequency and vibrational frequency shift

Fujii et al. reported, using experimental infrared (IR) spectroscopy, that the asymmetric C−H stretching vibration of the acetylene moiety exhibits a remarkable low-frequency shift (red shift) upon the cluster formation with the aromatic molecules [41]. Since one has an experimental evidence for benzene-acetylene complex, we decided to provide the data of C−H stretching frequencies with their intensities and the frequency shift for both acetylene and the aromatic systems forming the complex. Table 2 lists the above-mentioned data. For **1A**, the asymmetric C−H stretching frequency of acetylene is red-shifted by 17 cm^{-1} compared to the bare acetylene and this is in good agreement with the experimental report of the red-shift of 22 cm^{-1} [41]. It is worth mentioning that the calculated intensity of the corresponding frequency is considerably larger compared to free acetylene. Unlike the small value of red-shift of 2.3 cm^{-1} reported at the MP2/6-31G(d) level [43], the magnitude of the red-shift (17 cm^{-1}) obtained at the M06-2X/6-311+G(d,p) level is relatively large and close to the experimental value of 22 cm^{-1}. Similar to previous studies [41, 45], we observe a concomitant increase of bond length (by 0.003 Å) of interacting C−H bond of acetylene upon formation of the complex **1A** (see Fig. 1). Fujii et al. also mentioned that the C−H stretching frequencies of benzene were hardly perturbed by cluster formation with acetylene [41]. In line with the experimental observation [41], the computed data reveal very small blue-shift (2–4 cm^{-1}) for the benzene C−H stretching frequencies in case of **1A**. Interestingly, the C−H stretching frequencies of benzene in complexes **1B** and **1C** are red-shifted to a small extent, compared to free benzene. Such characteristic IR frequency shifts will be useful for experimentalists in identifying the complexes of **1B** and **1C** where the interactions of hydrogen atom(s) of benzene with the π-electron cloud of acetylene occur. As shown in Fig. 1, the bond lengths of interacting C−H bonds of benzene are not altered upon complex formation (for **1B** and **1C**). The C−H stretching frequencies of acetylene are red-shifted in **1B**, while they are blue-shifted in **1C** compared to the free acetylene.

In cases of **2A** and **2C**, one of the C−H stretching frequencies of TFB is considerably red-shifted compared to the corresponding C−H stretching frequency of the isolated species. The notable red-shifts (−26 and −24 cm^{-1}) observed for these configurations could be attributed to the interaction of H atom of TFB with the π-cloud of acetylene. The length of C−H bond of TFB involved in C−H···π interaction with acetylene is slightly elongated as expected for the red-shift. Interestingly, the C−H stretching frequencies of acetylene in **2A** are also considerably red-shifted (−18 and −16 cm^{-1}), with simultaneous elongation of the C−H bonds. This could be reasoned to the strong C−H···F hydrogen bond in addition to the C−H···π interaction (H atom of TFB interacts with acetylene). Though, C−H stretching frequencies of acetylene in **2B** and **2C** are red-shifted, the magnitudes of the shifts are smaller compared to **2A**. Similar to **1A**, the C−H stretching frequencies of aromatic moiety in **2B** are slightly blue-shifted. However, C−H stretching frequencies of acetylene in **2B** are red-shifted compared to the free molecule. It should be noted that the magnitudes of red-shifts in **2B** are smaller (4 and 3 cm^{-1}) than the case of **1A** (17 and 11 cm^{-1}). The vibrational frequency data indicate that three configurations for 1,3,5-trifluorobenzene-acetylene complex could be easily distinguished. The asymmetric C−H stretching frequency of acetylene is IR active. The intensity of this frequency tremendously increased upon forming complexes of same type **1A**, **2B** and **3B**. It remains similar in **2B** and **3B**, but **1A** has quite larger intensity than these two complexes.

Table 2 C−H stretching frequencies ($\nu_{C\text{-}H}$, in cm^{-1}), intensities (Int. in km/mol), and frequency shifts ($\Delta\nu$, in cm^{-1}) for the complexes and the corresponding frequencies and intensities for the individual fragments obtained at the M06-2X/6-311+G(d,p) level. See Fig. 1 for nomenclature of the complexes and **Ac** means acetylene

	$\nu_{C\text{-}H}$	Int.	$\nu_{C\text{-}H}$	Int.	$\Delta\nu^a$	$\nu_{C\text{-}H}$	Int.	$\Delta\nu^a$	$\nu_{C\text{-}H}$	Int.	$\Delta\nu^a$	$\nu_{C\text{-}H}$	Int.	$\Delta\nu^a$	$\nu_{C\text{-}H}$	Int.	$\Delta\nu^a$
			1A			**1B**			**1C**								
1 C−H	3181	(0)	3185	(0)	4	3178	(0.3)	−3	3175	(0.8)	−6						
1 C−H	3191	(0)	3194	(0)	3	3186	(0.3)	−5	3184	(0)	−7						
1 C−H	3191	(0)	3194	(0)	3	3190	(1)	−1	3187	(8)	−4						
1 C−H	3205	(18)	3208	(12)	3	3201	(18)	−4	3198	(18)	−7						
1 C−H	3205	(18)	3208	(12)	3	3202	(12)	−3	3201	(4)	−4						
1 C−H	3215	(0)	3217	(0.2)	2	3211	(1)	−4	3210	(2)	−5						
Ac C−H	3434	(101)	3417	(218)	−17	3429	(103)	−5	3445	(105)	11						
Ac C−H	3543	(0)	3532	(2)	−11	3538	(0.6)	−5	3546	(0)	3						
			2A			**2B**			**2C**								
2 C−H	3238	(0)	3212	(34)	−26	3241	(0)	3	3214	(45)	−24						
2 C−H	3239	(9)	3244	(6)	5	3242	(12)	3	3244	(5)	5						
2 C−H	3239	(9)	3252	(7)	13	3242	(12)	3	3248	(6)	9						
Ac C−H	3434	(101)	3416	(115)	−18	3430	(175)	−4	3429	(104)	−5						
Ac C−H	3543	(0)	3527	(0.5)	−16	3540	(3)	−3	3538	(0)	−5						
			3A			**3B**			**3C**			**3D**			**3E**		
3 C−H	3176	(0)	3175	(0)	−1	3177	(0)	1	3175	(0)	−1	3175	(0)	−1	3165	(3)	−11
3 C−H	3176	(2)	3175	(2)	−1	3177	(2)	1	3176	(2)	0	3176	(2)	0	3166	(0)	−10
3 C−H	3177	(1)	3176	(1)	−1	3178	(1)	1	3176	(1)	−1	3176	(0.2)	−1	3167	(8)	−10
3 C−H	3177	(0)	3176	(0)	−1	3178	(0)	1	3176	(0)	−1	3176	(4)	−1	3167	(3)	−10
3 C−H	3181	(1)	3178	(0.7)	−3	3181	(0.7)	0	3180	(0.4)	−1	3180	(2)	−1	3185	(1)	4
3 C−H	3181	(0)	3178	(0)	−3	3181	(0)	0	3184	(0)	−3	3180	(0)	−1	3185	(0.5)	4
3 C−H	3193	(8)	3192	(6)	−1	3193	(7)	0	3192	(10)	−1	3191	(7)	−2	3196	(13)	3
3 C−H	3193	(0)	3192	(0)	−1	3194	(0)	1	3192	(0)	−1	3192	(3)	−1	3196	(1)	3
3 C−H	3194	(0)	3193	(0)	−1	3194	(0)	0	3193	(0)	−1	3193	(2)	−1	3196	(17)	2
3 C−H	3194	(43)	3193	(43)	−1	3194	(40)	0	3193	(44)	−1	3192	(23)	−2	3201	(19)	7
3 C−H	3198	(34)	3195	(36)	−3	3198	(32)	0	3197	(21)	−1	3195	(35)	−3	3202	(18)	4
3 C−H	3198	(0)	3195	(0)	−3	3198	(0)	0	3197	(1)	−1	3197	(0.3)	−1	3205	(0.2)	7
Ac C−H	3434	(101)	3421	(48)	−13	3427	(172)	−7	3428	(101)	−6	3425	(103)	−9	3429	(102)	−5
Ac C−H	3543	(0)	3530	(0.1)	−13	3538	(1)	−5	3537	(2)	−6	3534	(2)	−9	3538	(1)	−5

[a]Difference of harmonic C-H stretching frequency in the complex minus the corresponding frequency in the free molecule: a negative value indicates red-shift and a positive value indicates blue-shift

Though the C−H stretching frequencies of acetylene in all the configurations from **3A** to **3E** are red-shifted compared to free acetylene, they are red-shifted slightly larger in **3A** than in other four configurations. In all the configurations, the C−H bond lengths of acetylene are slightly increased or no change is observed compared to the free acetylene. We neglect **3E** and **3F** from the discussion since those structures possess one imaginary frequency. It is worth mentioning that the intensity of asymmetric C−H stretching frequency of acetylene in **3A** is substantially smaller than that in free acetylene and other complex structures. The C−H stretching frequency data and the vibrational frequency shifts provided in Table 2 will aid experimentalists to characterize different configurations of complexes studied in this paper. Like in the case of benzene dimer [32, 33, 35, 36], different configurations of these complexes may be found experimentally.

Conclusions

In this study, we examined the strength of C−H···π interactions of two possible types for benzene-acetylene, 1,3,5-trifluorobenzene-acetylene and coronene-acetylene complexes using M06-2X/6-31+G(d,p) and M06-2X/6-311+G(d,p) computational approaches. Configurations **1A**, **2B**, **3B** and **3F** have the C−H···π interactions of same type (H of acetylene binds directly above the center of aromatic six-

membered ring). Among these four structures, the prototype benzene-acetylene complex (**1A**) shows stronger binding than other three. The binding energy of 2.91 kcal/mol calculated at the M06-2X/6-311+G(d,p) level for **1A** is in very good agreement with the experimental binding energy of 2.7±0.2 kcal/mol for benzene-acetylene complex [44]. In case of 1,3,5-trifluorobenzene-acetylene complex, **2A** exhibits stronger complexation energy than **2B** and **2C** because of the existence of both C−H···π and C−H···F hydrogen bonds. Owing to both π-π and C−H···π interactions, the structure **3A** is substantially more stable than other configurations in the pool of coronene-acetylene complexes. The classical T-shaped configuration formed by the C−H of acetylene interacting with central ring of coronene (**3B**) and the edge ring of coronene (**3F** structure) are considerably less stable than **3A**. The pictures of molecular electrostatic potentials obtained for the ligands are used to explain the binding strengths of different complexes. In agreement with experimental report [41], the asymmetric C−H stretching frequency of acetylene in **1A** is red-shifted by 17 cm^{-1} compared to the bare acetylene. For the lowest energy configuration of **2A** in TFB-acetylene complex, we obtained notable red-shift for one of the C−H stretching frequencies of 1,3,5-trifluorobenzene and the C−H stretching frequencies of acetylene. The C−H stretching frequencies of acetylene in all the configurations (from **3A** to **3E**) are red-shifted compared to free acetylene. However, they are red-shifted slightly larger in the lowest-energy structure **3A** than in other four configurations.

Acknowledgments We thank the National Science Foundation (NSF/CREST HRD-0833178) for financial support. Mississippi Center for Supercomputing Research (MCSR) is acknowledged for generous computational facilities.

References

1. Johnson ER, Keinan S, Mori-Sánchez P, Contreras-García J, Cohen AJ, Yang W (2010) J Am Chem Soc 132:6498–6506
2. Lee EC, Kim D, Jurečka P, Tarakeshwar P, Hobza P, Kim KS (2007) J Phys Chem A 111:3446–3457
3. Muller-Dethlefs K, Hobza P (2000) Chem Rev 100:143–168
4. Chipot C, Jaffe R, Maigret B, Pearlman DA, Kollman PA (1996) J Am Chem Soc 118:11217–11224
5. Ranganathan D, Haridas V, Gilardi R, Karle IL (1998) J Am Chem Soc 120:10793–10800
6. Brandl M, Weiss MS, Jabs A, Sühnel J, Hilgenfeld R (2001) J Mol Biol 307:357–377
7. Toth G, Murphy RF, Lovas S (2001) Protein Eng 14:543–547
8. Umezawa Y, Tsuboyama S, Takahashi H, Uzawa J, Nishio M (1999) Bioorg Med Chem 7:2021–2026
9. Li R, Dong H, Zhan X, Li H, Wen S, Deng W, Han K, Hu W (2011) J Mater Chem 21:11335–11339
10. Dinadayalane TC, Leszczynski J (2010) Struct Chem 21:1155–1169
11. Tauer TP, Derrick ME, Sherrill CD (2005) J Phys Chem A 109:191–196
12. Kwac K, Lee C, Jung Y, Han J, Kwak K, Zheng J, Fayer MD, Cho M (2006) J Chem Phys 125:244508
13. Dinadayalane TC, Gorb L, Simeon T, Dodziuk H (2007) Int J Quantum Chem 107:2204–2210
14. Dinadayalane TC, Gorb L, Dodziuk H, Leszczynski J (2005) AIP Conf Proc 786:436–439
15. Dinadayalane TC, Leszczynski J (2009) J Chem Phys 130:081101
16. Dinadayalane TC, Leszczynski J (2009) Struct Chem 20:11–20
17. Dinadayalane TC, Hassan A, Leszczynski J (2012) Theor Chem Acc 131:1131
18. Dinadayalane TC, Hassan A, Leszczynski J (2010) J Mol Struct 976:320–323
19. Dinadayalane TC, Afanasiev D, Leszczynski J (2008) J Phys Chem A 112:7916–7924
20. Hassan A, Dinadayalane TC, Leszczynski J (2007) Chem Phys Lett 443:205–210
21. Politzer P, Riley KE, Bulat FA, Murray JS (2012) Comput Theor Chem 998:2–8
22. Politzer P, Murray JS (2012) Theor Chem Acc 131:1114
23. Riley KE, Murray JS, Fanfrlik J, Rezac J, Sola RJ, Concha MC, Ramos FM, Politzer P (2011) J Mol Model 17:3309–3318
24. Meyer-Wegner F, Lerner HW, Bolte M (2010) Acta Cryst C66: o182–o184
25. Sinnokrot MO, Sherrill CD (2006) J Phys Chem A 110:10656–10668
26. Sinnokrot MO, Sherrill CD (2004) J Phys Chem A 108:10200–10207
27. Sinnokrot MO, Valeev EF, Sherrill CD (2002) J Am Chem Soc 124:10887–10893
28. Tsuzuki S, Honda K, Uchimaru T, Mikami M, Tanabe K (2002) J Am Chem Soc 124:104–112
29. DiStasio RA Jr, Helden GV, Steele RP, Head-Gordan M (2007) Chem Phys Lett 437:277–283
30. Janowski T, Pulay P (2007) Chem Phys Lett 447:27–32
31. Park YC, Lee JS (2006) J Phys Chem A 110:5091–5095
32. Arunan E, Gutowsky HS (1993) J Chem Phys 98:4294–4296
33. Steed JM, Dixon TA, Klemperer W (1979) J Chem Phys 70:4940–4946
34. Wang W, Pitoňák M, Hobza P (2007) ChemPhysChem 8:2107–2111
35. Erlekam U, Frankowski M, Meijer G, Helden GV (2006) J Chem Phys 124:171101
36. Erlekam U, Frankowski M, Helden GV, Meijer G (2007) Phys Chem Chem Phys 9:3786–3789
37. Hobza P, Havlas Z (2000) Chem Rev 100:4253–4264
38. Shibasaki K, Fujii A, Mikami N, Tsuzuki S (2006) J Phys Chem A 110:4397–4404
39. Ringer AL, Figgs MS, Sinnokrot MO, Sherrill CD (2006) J Phys Chem A 110:10822–10828
40. Ramos C, Winter PR, Stearns JA, Zwier TS (2003) J Phys Chem A 107:10280–10287
41. Fujii A, Morita S, Miyazaki M, Ebata T, Mikami N (2004) J Phys Chem A 108:2652–2658
42. Boese R, Clark T, Gavezzotti A (2003) Helvetica Chimica Acta 86:1085–1100
43. Donoso-Tauda O, Jaque P, Santos JC (2011) Phys Chem Chem Phys 13:1552–1559
44. Shibasaki K, Fujii A, Mikami N, Tsuzuki S (2007) J Phys Chem A 111:753–758
45. Mishra BK, Karthikeyan S, Ramanathan V (2012) J Chem Theory Comput 8:1935–1942
46. Sundararajan K, Viswanathan KS, Kulkarni AD, Gadre SR (2002) J Mol Struct 613:209–222
47. Granatier J, Lazar P, Prucek R, Šafářová K, Zbořil R, Otyepka M, Hobza P (2012) J Phys Chem C 116:14151–14162
48. Kysilka J, Rubeš M, Grajciar L, Nachtigall P, Bludský O (2011) J Phys Chem A 115:11387–11393
49. Zhao Y, Truhlar DG (2008) J Phys Chem C 112:4061–4067

50. Frisch MJ, Trucks GW, Schlegel HB, Scuseria GE, Robb MA, Cheeseman JR, Scalmani G, Barone V, Mennucci B, Petersson GA, Nakatsuji H, Caricato M, Li X, Hratchian HP, Izmaylov AF, Bloino J, Zheng G, Sonnenberg JL, Hada M, Ehara M, Toyota K, Fukuda R, Hasegawa J, Ishida M, Nakajima T, Honda Y, Kitao O, Nakai H, Vreven T, Montgomery JA Jr, Peralta JE, Ogliaro F, Bearpark M, Heyd JJ, Brothers E, Kudin KN, Staroverov VN, Kobayashi R, Normand J, Raghavachari K, Rendell A, Burant JC, Iyengar SS, Tomasi J, Cossi M, Rega N, Millam JM, Klene M, Knox JE, Cross JB, Bakken V, Adamo C, Jaramillo J, Gomperts R, Stratmann RE, Yazyev O, Austin AJ, Cammi R, Pomelli C, Ochterski JW, Martin RL, Morokuma K, Zakrzewski VG, Voth GA, Salvador P, Dannenberg JJ, Dapprich S, Daniels AD, Farkas Ö, Foresman JB, Ortiz JV, Cioslowski J, Fox DJ (2010) Gaussian 09, Revision C.01. Gaussian, Inc, Wallingford
51. Boys SF, Bernardi F (1970) Mol Phys 19:553–566
52. Spartan '10, Wavefunction, Inc. Irvine, CA.
53. Shao Y, Molnar LF, Jung Y, Kussmann J, Ochsenfeld C, Brown ST, Gilbert ATB, Slipchenko LV, Levchenko SV, O'Neill DP, DiStasio RA Jr, Lochan RC, Wang T, Beran GJO, Besley NA, Herbert JM, Lin CY, Van Voorhis T, Chien SH, Sodt A, Steele RP, Rassolov VA, Maslen PE, Korambath PP, Adamson RD, Austin B, Baker J, Byrd EFC, Dachsel H, Doerksen RJ, Dreuw A, Dunietz BD, Dutoi AD, Furlani TR, Gwaltney SR, Heyden A, Hirata S, Hsu C-P, Kedziora G, Khalliulin RZ, Klunzinger P, Lee AM, Lee MS, Liang WZ, Lotan I, Nair N, Peters B, Proynov EI, Pieniazek PA, Rhee YM, Ritchie J, Rosta E, Sherrill CD, Simmonett AC, Subotnik JE, Woodcock HL III, Zhang W, Bell AT, Chakraborty AK, Chipman DM, Keil FJ, Warshel A, Hehre WJ, Schaefer HF, Kong J, Krylov AI, Gill PMW, Head-Gordon M (2006) Phys Chem Chem Phys 8:3172–3191
54. Morita S, Fujii A, Mikami N, Tsuzuki S (2006) J Phys Chem A 110:10583–10590
55. Hohenstein EG, Duan J, Sherrill CD (2011) J Am Chem Soc 133:13244–13247
56. Sinnokrot MO, Sherrill CD (2004) J Am Chem Soc 126:7690–7697
57. Sinnokrot MO, Sherrill CD (2003) J Phys Chem A 107:8377–8379
58. Wheeler SE (2011) J Am Chem Soc 133:10262–10274
59. Wheeler SE, McNeil AJ, Müller P, Swager TM, Houk KN (2010) J Am Chem Soc 132:3304–3311
60. Wheeler SE, Houk KN (2008) J Am Chem Soc 130:10854–10855